PREPRINT UCRL- 77323

Lawrence Livermore Laboratory

THERMAL DEPLETION OF A GEOTHERMAL RESERVOIR WITH BOTH FRACTURE AND PORE PERMEABILITY

P. W. Kasameyer and R. C. Schroeder

August 10, 1976

This paper was prepared for submittal to the Journal of Geophysical Research

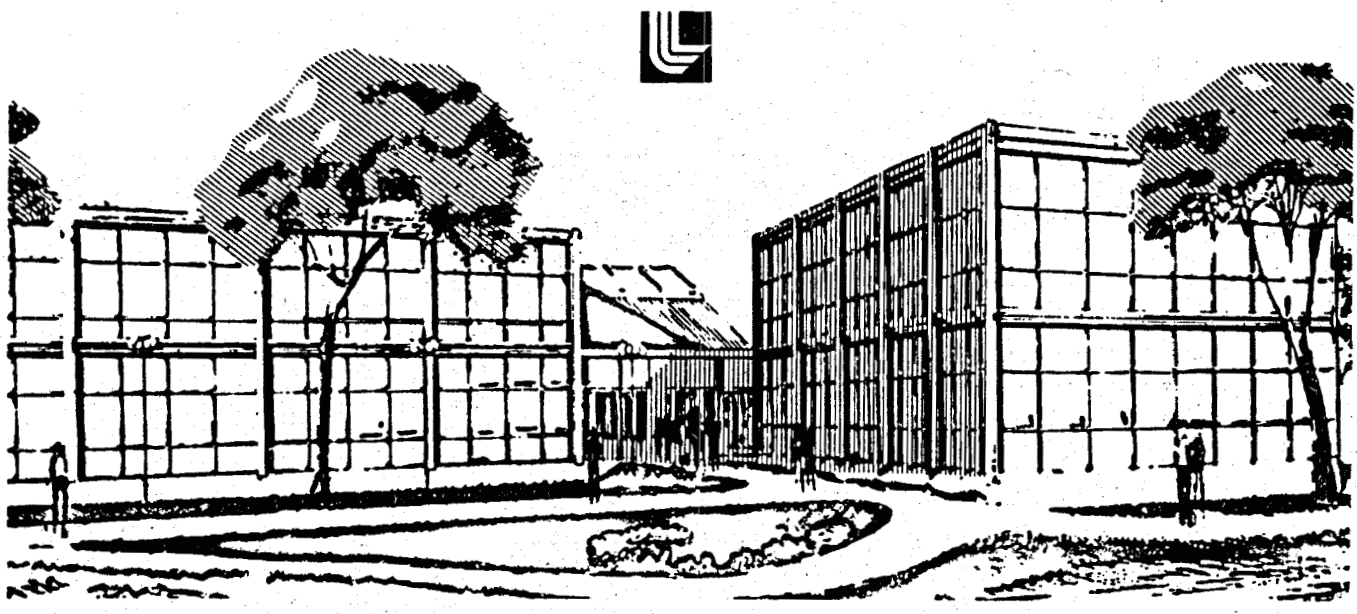

DISCLAIMER

THERMAL DEPLETION OF A GEOTHERMAL RESERVOIR WITH BOTH FRACTURE AND PORE PERMEABILITY

P. W. Kasameyer and R. C. Schroeder*

Lawrence Livermore Laboratory, University of California
Livermore, California 94550

ABSTRACT

The useful lifetime of a geothermal resource is often calculated from the volume of available hot water. The lifetime may actually be longer if reinjected fluid is heated by the rock matrix and produced again. For reservoirs containing only porous material and for reservoirs consisting entirely of fractured impermeable rock, that extended lifetime has been estimated. We present here a method for estimating the useful lifetime of a reservoir in porous rock where the injection and production wells intersect a fracture system. Equations are derived for the pore-fluid and fracture-fluid temperatures averaged over large regions of the geothermal field. Problems such as incomplete areal sweep and interfingering of cool and hot fluids are ignored. We develop approximate equations relating average temperatures to the heat flowing from rock to fluid, and we justify their use by comparing our results with solutions of the exact equations. Our equations for the temperature decline can be solved quickly.

In our model, fractures are characterized by three parameters: aperture w, permeability k_{fr}, and spacings between fractures D. For certain values of these parameters, cool reinjected fluid in fractures may reach the production wells long before all the warm pore fluid has been tapped, shortening the useful lifetime of the field. We ignore the traditional

*Present address: Lawrence Berkeley Laboratory, Berkeley, California 94720.

(and important) problems of reservoir engineering, flow rate determination, drawdown, sweep patterns, etc. Thus, our results are most useful in providing a correction factor which can be applied to lifetime estimates obtained from a detailed simulation of a field assuming porous rock. That correction factor is plotted for clean fractures ($k_{fr} = w^2/12$) as a function of w and D for several lifetime ranges.

Small-scale fractures seen in cores from the Salton Sea Geothermal Field are too closely spaced to reduce lifetime estimates. However, large-scale fault systems exist within that field, and they are attractive drilling targets because they produce large flow rates. If large scale faults communicate between injection and production wells, they may reduce the useful lifetime of those wells.

INTRODUCTION

Various means have been developed in the gas and oil industry for modeling reservoir depletion. Mathews and Russell [1967] discuss well-testing models used to extrapolate production data to abandonment conditions, and Ramey (personal communication, 1973) describes superimposed transient well-flow solutions to extrapolate for the approximate lifetime of a field. But these are isothermal methods and cannot be used for geothermal depletion estimates. Whiting and Ramey [1969] use least-squares fitting techniques in conjunction with a material- and heat-balance model to obtain estimates for production parameters from which the subsequent behavior of a geothermal field can be extrapolated. Their method was used to model the Wairakei geothermal area, but, unfortunately, it is not applicable before a resource has been developed and produced. Another alternative is to use a large digital computer to simulate the differential equations which model in detail the coupled heat- and mass-transfer phenomena within a reservoir [Brownell et al., 1975; Lasseter et al., 1975; Mercer, 1973]. Simulation requires a large effort, and it is costly. Also, all available models apply only to homogeneous porous media and not to formations with distributed fractures. Gringarten, Witherspoon, and Ohnishi [1975] have computed the amount of heat extracted from hot, impermeable fractured rock as a function of time. Bodvarsson [1974] treats the limiting cases of rock made up entirely of small pores, or entirely of impermeable fractured rock.

In this paper, we outline a model for estimating the thermal depletion of a liquid-dominated reservoir in porous, permeable rock with distributed fractures. Numerical solution of the equations for this model requires less computer time than the simulations mentioned above, because of two

approximations. Equations are written for the average temperature over large regions of the reservoir, and the total heat transfer between rock and fluid in each region is expressed in terms of those average temperatures. Simplifying assumptions are chosen so that an exact solution would give the maximum possible lifetime for the reservoir, accounting for the heat flow from the rock. The extent that our approximate solutions underestimate that maximum is discussed when results are presented.

DEFINITION OF THE PROBLEM

A finite, liquid-dominated geothermal system in porous, permeable rock with distributed fractures, has an initial temperature T_0. Fluid is removed from the reservoir through production wells and replenished at temperature T_{ref} through reinjection wells or by recharge of cool fluid from adjacent rocks. A distribution of wells is assumed to exist which sweeps out the field completely, and which can produce and maintain a specified mass flow rate q. The particular well pattern need not be specified since there is no unique pattern which will produce perfect sweep. The heat depletion processes for the reservoir are indicated in Figure 1.

We want to determine the temperature in the production wells as a function of time. Conceptually, the reservoir is divided into M regions of equal volume, whose boundaries coincide with flow fronts of the reinjected fluid. Region 1 consists of unconnected cylinders around the injection wells, or areas near the boundaries of the reservoir where recharge occurs. Region M consists of several unconnected cylinders about the production wells. Within the reservoir, the fluid flows sequentially through the regions, as indicated in Figure 2. Knowledge of the particular well

locations is not necessary for solution of the problem, and the boundaries need not be specified.

Three steps are followed to determine the temperature in the production well as a function of time:

(1) Dimensionless heat-balance equations are written for each region, relating the average temperature of the fracture fluid and saturated rock within the region.

(2) A rock model that allows a simple expression relating the rock/fluid heat transfer to the average component temperatures is chosen.

(3) The resulting coupled differential equations are solved numerically by holding the coefficients constant and using the analytical solution during appropriately short time intervals.

The production well temperature is calculated from the fracture- and pore-fluid temperatures in the M^{th} region.

COUPLED RATE EQUATIONS FOR HEAT DEPLETION IN EACH REGION

We write the heat balance equations for the average fracture-fluid temperature T_{fr} and the average saturated rock temperature T_s in a region under the following assumptions:

(1) The two fluid components, fracture and pore fluid, do not mix within the region.

(2) The mass of each fluid component within the region is constant.

(3) The rates q_{fr} and q_p at which the two fluid components flow through the region are determined from the total mass flow rate at the wells and from the rock model.

(4) The fluids enter each region at a temperature determined by the previous

region, and they leave with the average temperature T_{fr} or T_s of that region.

(5) The pore fluid and rock matrix are assumed to come to the same temperature rapidly compared to the rate at which fluid moves in the pores.

(6) Conduction of heat from the region is ignored.

(7) The saturated rock and fracture fluid have constant heat capacities over the temperature range considered. The thermal masses of the two reservoir components (saturated porous rock and fracture fluid) are given by

$$\mu_s = \rho_s(1-\phi_{fr})V\ C_s$$
$$\mu_{fr} = \rho_f\phi_{fr}V\ C_f \qquad (1)$$

where

ϕ = porosity

ρ = density

V = volume of each region

C = specific heat capacity

Subscripts fr, s, and f refer to fracture, saturated rock, and fluid components, respectively. The heat content of each component is given by the product of the thermal mass and the difference between the given component temperature and T_{ref}.

(8) Pressure terms in the heat balance equation are neglected.

Given these assumptions, the heat balance equations relating the average temperatures of the fracture fluid and saturated rock in a region are written as

rate of change of heat = rate at which heat is removed from region by fluid flow + rate of exchange of heat from rock to fluid

$$\mu_{fr} \frac{dT_{fr}}{dt} = q_{fr} C_f (T_{fr} - T_{fr0}) + H(t, T_{fr}, T_s)$$

$$\mu_s \frac{dT_s}{dt} = q_p C_f (T_s - T_{s0}) - H(t, T_{fr}, T_s) \qquad (2)$$

The model definition allows the input temperatures of a region (T_{fr0}, T_{s0}) to be either the appropriate component temperature from the adjacent region or a mixture of the two components from the adjacent region. The heat transfer term H depends on the rock model chosen.

To express equations (2) in dimensionless form, we normalize the temperature, time, and heat transfer rate:

$$T^* = \frac{T - T_{ref}}{T_0 - T_{ref}} \quad , \quad t^* = \alpha t \quad , \quad H^* = \frac{H}{\mu_{fr} \alpha (T_0 - T_{ref})} \qquad (3)$$

where α is the rate constant for the diffusion of heat into the fractures. That rate constant is defined below for our particular rock model. Three dimensionless groupings that have physical significance appear in the modified equations,

$$\theta^* = \frac{\alpha(\mu_s + \mu_{fr})}{q C_f} \quad , \quad R_q = \frac{q_{fr}}{q_P} \quad , \quad R_\mu = \frac{\mu_{fr}}{\mu_s} \qquad (4)$$

The constant θ^* is the ratio of the heat contained in the region to the rate at which heat is removed by fluid flow. The flow and thermal mass ratios are determined by the rock model.

The dimensionless form of (2) for the change in the average temperatures in a region as a function of time is then given by:

$$\frac{dT^*_{fr}}{dt^*} = -\frac{R_q(1+R_\mu)}{R_\mu(1+R_q)}\frac{1}{\theta^*}(T^*_{fr} - T^*_{fr0}) + H^*(t^*, T^*_{fr}, T^*_s)$$

$$\frac{dT^*_s}{dt^*} = -\frac{(1+R_\mu)}{(1+R_q)}\frac{1}{\theta^*}(T^*_s - T^*_{s0}) - R_\mu H^*(t^*, T^*_{fr}, T^*_s) \qquad (5)$$

THE ROCK AND HEAT-TRANSFER MODELS

Within each region of the reservoir, the medium is modeled as a sandwich of slabs of porous rock separated by planar fractures perpendicular to the axes of the wells (see Figure 3a). The fractures have an aperture w and a center-to-center spacing D. Thus, the fracture porosity is $\phi_{fr} = w/D$.

The fluid flows parallel to the fractures within the region, and leakage into the fractures within a region is ignored. Fractures perpendicular to the flow direction are modeled by allowing the pore and fracture fluids to mix at the outlet of the regions. Heat conduction from the porous rock to the fluid is ignored in fractures perpendicular to the flow. (That contribution to the heat flow could be accounted for by adding a "tortuosity" factor in the equations.) From our rock model, we see that in the reservoir,

$$R_q = \frac{k_{fr}w}{k_p(D-w)} \qquad (6)$$

where k_p and k_{fr} are the rock and fracture permeabilities. The fractures are assumed to be perpendicular to the wells, so the ratio of the flow into the well bore from the fractures and from the pores will also be R_q. (Modification of the results for fractures at other angles to the well bore is discussed in the section labeled Discussion.) For the calculations described below, we assume that the permeability of the fractures is equal to $w^2/12$.

That expression has been derived for a smooth, planar channel [Lamb, 1932]. Different values of k_{fr} could be used to estimate the effect of "dirty" fractures or rubble-filled fault zones.

The dimensionless heat transfer term H^* within a given region is calculated by dividing the rock slabs between fractures into smaller rectangular blocks with edge dimensions A, B and (D-w), as shown in Figure 3b. The heat transfer from the saturated rock to the fracture fluid will be summed over all the small blocks in all the slabs within a region. The size of the block is defined to be small enough so that the pore fluid and rock temperatures do not vary significantly in the flow direction within a block. No particular values are chosen for A and B because they cancel out of all expressions. Each region has a volume V and contains N blocks, where

$$N = \frac{V}{ABD} \tag{7}$$

The temperatures in the block are $\hat{T}_{fr}$ and $\hat{T}_s$.

In general, the heat transfer term H^* depends on the integral of the entire history of the temperature, or equivalently, on the spatial distribution of temperature within the region. Rather than solve a complicated integral-differential equation, we use our model of the rock to approximate the heat transfer term by an expression depending only on the instantaneous average temperatures $\hat{T}_{fr}$ and $\hat{T}_s$ within the region. Different approximations are used for early and late times.

For early times, we approximate the heat flow from each block using the solution for the temperature in a solid bounded by infinite parallel planes that have been held at constant temperature. The total heat conducted from the rock block (in the time interval from 0 to t^*) is overestimated by using the amount which would have been transferred had the fracture fluid been at

the temperature $\hat{T}^*_{fr}(t^*)$ since $t^* = 0$. The actual heat transfer must be less, because the fluid temperature must have decreased monotonically from 1 at $t^* = 0$ to $\hat{T}^*_{fr}(t^*)$.

For this approximation, the solution for the average temperature of the rock block at time t^* is given by Carslaw and Jaeger [1959 (Sec. 3.3, Eq. 1.1)]. The series solution that converges at early times is used:

$$\hat{T}^*_s - \hat{T}^*_{fr} = (1-\hat{T}^*_{fr}) \left\{1-2\sqrt{t^*}\left[\frac{1}{\sqrt{\pi}} + 2\sum_{n=1}^{\infty}(-1)^n \text{ierfc}\left(\frac{n}{\sqrt{t^*}}\right)\right]\right\} \quad (8)$$

where ierfc(x) is the integrated complementary error function, and the parameter α is now defined in terms of the physical constants by

$$t^* = \alpha t = \frac{4\lambda_s}{[D-w]^2} t \quad (9)$$

$\lambda_s = K_s/\rho_s C_s$ is the thermal diffusivity of the saturated rock.

For early times ($t^* < \pi/16$), the summation in (8) is negligible; thus the dimensionless heat transfer rate for a single rock block is

$$\hat{Q}^*_{early} = \frac{\hat{Q}_{early}}{\alpha\mu_{fr}(T_0-T_{ref})} \quad (10)$$

where

$$\hat{Q}_{early} = -\frac{d}{dt}\left[\rho_s C_s ABD\,(1-\phi_{fr})T_s(t)\right] \quad (11)$$

From the definition of μ_{fr} in (1) and from (7) and (10),

$$\hat{Q}^*_{early} = -\frac{1}{NR_\mu}\frac{d\hat{T}^*_s}{dt^*} = \frac{1}{NR_\mu}\left[(1-\hat{T}^*_{fr})\frac{1}{\sqrt{\pi t^*}} - 2\sqrt{\frac{t^*}{\pi}}\frac{d\hat{T}^*_{fr}}{dt^*}\right] \quad (12)$$

In a similar manner, we define the late dimensionless heat transfer (for $t^* > 1$) by

$$\hat{Q}^*_{late} = \frac{\hat{Q}_{late}}{\mu_{fr}\alpha(T_0-T_{ref})} \tag{13}$$

where

$$\hat{Q}_{late} = \frac{(2AB)4K_s}{(1-\phi_{fr})D}(\hat{T}_s-\hat{T}_{fr}) \tag{14}$$

is the heat flow that would result from a constant temperature gradient in the rock. Here (2AB) is the block area through which heat is transferred. This gives

$$\hat{Q}^*_{late} = \frac{2}{NR_\mu}(\hat{T}^*_s - \hat{T}^*_{fr}) \tag{15}$$

For the intermediate times ($\pi/16 < t^* < 1$), interpolated values are used. We define an interpolation function $F(t^*)$ such that

$$\begin{aligned} F(t^*) &= 1 && t^* < \pi/16 \\ &= \left(\frac{t^*-1}{\pi/16-1}^{\,2}\right) && \pi/16 < t^* < 1 \\ &= 0 && t^* > 1 \end{aligned} \tag{16}$$

Different interpolating functions (t^*, t^{*2}, and $1-\cos t^*$) change the output temperature by less than a few percent. Equation (16) was chosen because it produces the smoothest output temperature curve. Then the dimensionless transfer from the saturated rock block to the fracture fluid is approximated by

$$\hat{Q}^*(t^*) = F\,\hat{Q}^*_{early} + (1-F)\hat{Q}^*_{late}$$

$$= \frac{1}{NR_\mu}\left\{ F(t^*) \left[(1-\hat{T}^*_{fr})\frac{1}{\pi t^*} - 2\sqrt{\frac{t^*}{\pi}}\frac{d\hat{T}^*_{fr}}{dt^*}\right] \right.$$

$$\left. +2(1-F(t^*) \quad (\hat{T}^*_s - \hat{T}^*_{fr}) \right\} \tag{17}$$

The total dimensionless heat transfer H^* is obtained by summing over all N blocks in a region, i.e.

$$H^*(t^*, T^*_{fr}, T^*_s) = \sum^N \hat{Q}^*(t^*) \tag{18}$$

The average dimensionless temperatures of the two components are obtained by summing the average temperatures in a block and dividing by the number of blocks in a region (N). That is,

$$T^*_s = \frac{\sum^N T^*_s}{N}$$

$$T^*_{fr} = \frac{\sum^N T^*_{fr}}{N} \tag{19}$$

The total dimensionless rate equations for the change in temperature in a given region as a function of time are

$$\left(1+\frac{\beta_3}{R_\mu}\right)\frac{dT^*_{fr}}{dt^*} = -\frac{R_q}{R_\mu}\frac{(1+R_\mu)}{(1+R_q)}\frac{1}{\theta^*}(T^*_{fr} - T^*_{fr0}) + \frac{1}{R_\mu}[-(\beta_1+\beta_2)T^*_{fr}+\beta_2 T^*_s+\beta_1]$$

$$\frac{dT^*_s}{dt^*} = -\frac{(1+R_\mu)}{(1-R_q)}\frac{1}{\theta^*}(T^*_s - T^*_{s0}) + (\beta_1+\beta_2)T^*_s - \beta_2 T^*_s - \beta_1 + \beta_3\frac{\partial T^*_{fr}}{\partial t^*} \tag{20}$$

$$\beta_1 = \frac{F(t^*)}{\sqrt{\pi t^*}}$$

$$\beta_2 = 2(1-F(t^*))$$

$$\beta_3 = 2F(t^*)\sqrt{\frac{t^*}{\pi}}$$

The initial conditions (for all regions) are

$$T^*_{fr}(0) = T^*_s(0) = 1 \tag{21}$$

The variables T^*_{fr0} and T^*_{s0} represent the temperature of the fluid flowing into a region. For the first region, which is where injection occurs, $T^*_{fr0} = T^*_{s0} = 0$ for all time. If the two fluid components are allowed to mix in the fracture that separates regions, then

$$T^*_{fr0}(t^*) = T^*_{s0}(t^*) = \frac{T^*_s(t^*) + R_q T^*_{fr}(t^*)}{1+R_q} \tag{22}$$

If the fluids are not mixed between regions, then the input vlaues for a region are given by the output values for the adjacent region.

The solution of these dimensionless region equations depends on the four parameters: region number, θ^*, R_μ, and R_q. The independent variable is t^*, and the choice of mixing between regions, or not mixing, provides the final constraint. The depletion of the reservoir is given by the mixture temperature (equation 24) for region M.

THE SOLUTION OF THE COUPLED RATE EQUATIONS

The pair of coupled rate equations (20) for each region would have simple solutions if the input temperature to the region and the β_1 were constants. The appendix contains solutions of these equations, and the solutions consist of pairs of decaying exponentials. The actual equations have time-dependent coefficients. To solve them, we assume that the coefficients are constant over short periods of time. The solutions at the end of the short interval are used as the initial conditions for the next time interval, when the coefficients have new constant values. A step-function approximation for the output temperature of one volume is calculated, and

that step-function is used as the input for the next region.

Several criteria were used to choose time steps that produce an acceptable approximation at relatively low computation cost:

(1) The dimensionless input and output temperatures had to change by less than 0.01 during the time step.

(2) An output point had to be generated for every time interval greater than $M\theta^*/50$.

(3) The heat transfer coefficient had to change by less than 3% in any one timestep.

Applying these criteria results in smooth curves. The only distortion is that due to the changing heat transfer term near dimensionless time equal to 1, and this distortion appears only in problems where flow in the fractures dominates flow in the pores. Different interpolation methods could possibly be used to reduce this distortion, but they would not improve the accuracy of our model.

Our solution method is not the only method that could be applied, but most other methods suffer from an intrinsic problem with two-component flow when one of the component velocities greatly exceeds the other. That is, when the fracture flow rate is much greater than the pore flow rate, the time step must be determined by the highest velocity. This results in unacceptably short time steps and large numbers of calculational steps. The method described here avoids this problem.

It is important that the piecewise constant approximation of the output temperature be chosen as the <u>average</u> temperature within each time interval. Using either the maximum or minimum value will cause heat errors to accumulate from region to region.

COMPARISON OF OUR RESULTS TO PREVIOUS WORK

Our model has been derived to be applicable to problems involving both fracture and pore permeability. To demonstrate the strengths and weaknesses of the model and our associated solution process, a comparison is made between our results and the calculations published for the limiting cases of no fractures on the one hand and impermeable fractured rock on the other.

Bodvarsson [1974] showed that a hyperbolic equation results if there are no fractures and if conduction within the fluid is ignored. The solution of the equation is simple, i.e., $T = f(x + ut)$. A given initial temperature distribution propagates with no distortion at a velocity u slower than the fluid velocity by a factor equal to the ratio of the thermal masses of the fluid and the saturated rock. For our problem, the initial temperature distribution is constant for $x > 0$, and it is zero for $x < 0$. The analytical solution of the exact equation allows such a steep front to propagate with no distortion.

Homsy [1975] showed that any numerical solution must cause a diffusion of that steep temperature gradient, due to averaging of temperatures within the volumes used in the numerical solutions. The averaging causes the temperature jump to be smoothed out, and it allows cool fluid to reach the production wells too soon. The diffusion of the thermal front can be reduced by taking smaller volumes, and numerical methods have been devised to further reduce the diffusion (upstream weighting, time-splitting, etc.). Homsy shows that it is impractical to use a fine enough grid to eliminate the problem.

The effect of diffusion can easily be seen by comparing our numerical results to the analytical solution. If there are no fractures, $R_\mu = R_q = 0$, and the solution depends only on t^*, θ^*, and M. Solutions for two different

values of M are shown in Figure 4, where time is represented as a fraction of the time constant for the entire reservoir, $\tau^* = M\theta^*$. The analytical solution is a step function, but the numerical results have a smooth transition from 1 to 0. With 10 regions, the temperature begins to drop at $t^* = \tau^*/2$, and the temperature has fallen to 0.8 at $t^* - 3\tau^*/4$. A more abrupt temperature drop results if 100 regions are used in the calculation, so that $T^* = 0.8$ at $t^* = 0.9\tau^*$. All the results presented below are calculated for models with 10 regions, and the temperature decay starts early by a similar amount of time. Because our model is to be used mostly to compare relative decay times for different fracture parameters, the early temperature decline caused by the numerical method is not a serious problem.

Our results are compared with calculations for porous flow for another reason, i.e., to emphasize that we have calculated an unrealistically high upper bound for the total heat that may be removed from the rock. For example, our results (neglecting diffusion) suggest that all the heat can be removed from the rock by the reinjection (or recharge) process before any temperature decline occurs at the production well. It is important to emphasize again that many factors not included in our model will reduce the percentage of heat drawn from the rocks. These factors include incomplete sweep, pressure drawdown, and fingering or mixing of cool and hot fluid.

If there is flow only in fractures, $R_q \to \infty$ and the equations are specified by R_μ, θ^*, and M. We have approximated the heat conduction terms using a simplification for the early time that can be justified only if our equations produce results which compare favorably to calculations made using a more detailed heat-transfer model. Gringarten et al. [1975] have calculated the heat depletion for fracture flow in an impermeable rock matrix assuming that R_μ goes to zero. They solved the exact equation for this problem using

Laplace transforms, and then they evaluated their solution by a numerical inversion.

Their general results are compared with ours in Figure 5. Our calculations using the simplified heat transfer term agree with theirs to about 10% of the total temperature range. Our solutions have the following properties:

(1) At very early times ($t^* < \pi/16$), we overestimate the fracture fluid temperature, as was intended.

(2) At very late times (t^* greater than 2), the temperature front is diffused by averaging, and it is not as steep as the analytical solution requires. This effect can be reduced by including more sub-volumes, but the results as given are considered acceptable.

(3) Our results have kinks in the time periods where the heat transfer modeling method is changing, i.e., in the interpolation interval. These kinks have been discussed above, and could possibly be eliminated by a more detailed interpolation method.

THERMAL DEPLETION OF A RESERVOIR WITH COMBINED FRACTURE AND POROUS FLOW

In a permeable medium, fractures may allow a faster breakthrough of cool reinjection fluid than would be predicted using porous flow. An example of the effects of different fracture spacings on thermal depletion is seen on our calculated curves shown in Figure 6. The physical parameters (Table 1) and constant flow rate were chosen to represent power production at the Salton Sea Geothermal Field (SSGF) at a rate which corresponds to one complete production-injection cycle of the fluid in the field in 20 years [Towse, 1975]. A constant large fracture aperture w has been chosen so that the changes in depletion curves due to fracture spacing D will be dramatic.

For small fracture spacings, our solution for output temperature against time is the same as for totally porous rock. For this example, when $D < 10$ m, the rock is divided into small enough segments by the fractures to permit the heat to be conducted out of the rock in the length of time required to remove all the heat from the reservoir. The spacings for which the rock behaves as if the flow were in pores can be estimated from the diffusivity of the saturated rock.

If the fracture separation is increased, there are fewer fractures in a given volume, and the fluid velocity in each fracture increases. The heat cannot be conducted from the rock rapidly enough, and there is not enough flow from the pores to heat the fluid. Thus, the output temperature falls more rapidly than predicted by models of porous flow. However, if the fracture spacing (for this choice of parameters and power production) increases beyond 300 m, the lifetime increases because the volume of fracture fluid is small and the flow at the production well is primarily pore fluid, which cools slowly. From Figure 6, we see that fractures could reduce the useful lifetime of a field by a factor greater than 50 below a design lifetime based on porous flow calculations.

Our thermal depletion model can be used to estimate how the useful lifetime of a field will be reduced if fractures are present. Let τ be the time required to remove the heat from a particular geothermal field, calculated from a complicated simulation based on porous flow. Thermal depletion curves for any fracture aperture and spacing could be calculated for that field by choosing M, θ^*, and α such that $M\theta^*/\alpha = \tau$.

The reduction in reservoir lifetime caused by different combinations of aperture and spacing can be indicated on a single figure by contouring the time t_L at which the output temperature drops below the useful temperature

range. That temperature range would be determined by the power-generating equipment at any field. A contour plot of t_L as a function of D and w for a fixed τ would be useful for a single set of reservoir parameters such as those in Table 1. So that the plots we present can be used for many different applications, we contour t_L/τ as a function of R_q and R_μ. The contours apply to <u>any</u> set of parameters, if τ is scaled so as not to change R_μ, R_q, and τ^* for any point on the contours. Recall that if $k_{fr} = w^2/12$,

$$\tau^* = \alpha\tau = \frac{4\lambda_s}{(D-w)^2}\,\tau$$

$$R_\mu = \frac{\rho_F C_F}{\rho_s C_s}\,\frac{w}{(D-w)} \qquad (26)$$

$$R_q = \frac{w^3}{12k_p(D-w)}$$

We can express τ^* in terms of τ, R_μ, and R_q.

$$\tau^* = \frac{4R_\mu^3\lambda_s\tau}{12k_p R_q}\left(\frac{\rho_s C_s}{\rho_F C_F}\right)^3 \quad \tau = \text{constant} \qquad (27)$$

For example, a matrix permeability (k_p) of 10^{-13} m^2 was used to generate the figures below. If the matrix permeability of a reservoir is assumed to be 10^{-15} m^2, then the time constants for each figure must be multiplied by 100. New figures would have to be produced if the fracture permeability is not assumed to be $w^2/12$.

In Figure 7, the ratio t_L/τ has been contoured for three values of τ. The useful temperature range was assumed to end when the dimensionless temperature drops to 0.8. A realistic lifetime estimate is obtained by calculating R_q and R_μ for the given fracture-system parameters and multiplying the appropriate τ by the factor contoured in Figure 7. For many fracture

systems (small R_q or large R_μ), the lifetime is the same as that calculated for porous flow. (Our correction factor never exceeds 0.75, because of diffusion as discussed above.) For fracture distributions represented by the upper left-hand corner of Figure 7, the temperature at the production well may decline much more rapidly than predicted from porous-flow simulations.

APPLICATION TO THE SALTON SEA GEOTHERMAL FIELD (SSGF)

Cores obtained from the State #1 well in the SSGF show that the rock is broken by small-aperture fractures with spacings of less than 0.5 m. Lines of constant w and D for the field are shown in Figure 7d. The values of R_q and R_μ with no reduction of the lifetime are in the shaded area. We expect no significant reduction of lifetime due to fractures as closely spaced as those observed in the cores examined.

Fracture systems also exist on a much larger scale in the SSGF, however, and these systems may cause a rapid decline of the production fluid temperature. Helgeson [1968] states that

> ...open fractures have been intersected by a number of the wells. There is little doubt that these fractures serve as production zones for the wells. However, it is equally apparent (from selective production tests in the wells) that the geothermal brines are derived by the fractures from the pore spaces of the sand reservoir in the immediate geothermal area. At least two sets of fractures have been encountered to date, neither of which has undergone significant displacement. One of these is believed to contribute brine to five wells.

Randall [1974] and Towse and Palmer [1976] postulated several faults in the area to explain the variation in electric logs from adjacent wells. Hill et al. [1975] and Tien-Chang Lee (personal communication, 1976) have mapped earthquake epicenters indicating that at least one of the faults may be

active and may remain open in spite of chemical reactions with the brine. Meidav et al. [1976] have used a fault system to explain resistivity observa- observations near the field. All these lines of evidence indicate that permeable fractures with spacings greater than 100 m may exist in the SSGF.

From Figures 7b and 7d, we see that such a fracture system communicating between production and injection wells could cause a large decrease in the useful lifetime of the field if the fracture apertures are greater than a millimeter. Large-aperture systems are probably poorly modeled as clean planar fractures. Consequently, the contours in Figure 7 are not directly applicable for estimating the possible depletion due to such a system. If the permeability of the fracture zones can be estimated either from well tests or from a theoretical characterization of the rubble in the zone, then the decrease of the liftime due to those fractures can be calculated.

DISCUSSION

A model is an idealization of reality, and one must be aware of the limitations imposed by that idealization. Our description of the fracture system has two limitations: (1) the flow has been assumed to occur in fractures perpendicular to the wellbore, and (2) a very simple fracture system has been postulated.

The first idealization does not cause problems. Many fracture systems are nearly vertical in orientation and intersect wells at a high angle. The wells in our model were assumed to be perpendicular to the fractures so that we could calculate the ratio of fracture fluid to pore fluid flowing into a well. For high-angle fractures, there will be slightly more fracture fluid mixed into the well, and the output temperatures will be cooler than the upper limits calculated here. The effect would be very large only if the

fracture intersects the well bore over a long distance, and this is very unlikely.

It is difficult to assess the limitations imposed by the simplicity of our fracture model. A real rock might be described by a distribution function for pore space (and fracture) size, shape, and frequency. Our simple model assumes that the distribution functions are two delta functions, one for microscopic pores and one for macroscopic fractures. Distinct fractures are visible in porous rock cores from the Salton Sea Field. This suggests that the actual distributions may be bimodal. Future work might involve using a model with a broader distribution function for estimating the effect that a range of fracture parameters would have on the calculated results.

From our calculations, we have learned that the distribution of flow within the rock matrix is important for predicting thermal depletion. This knowledge is useful only if the distribution of flow in the reservoir rocks can be measured. Traditional procedures for measuring permeability from well testing must be supplemented by innovative techniques to estimate fracture system parameters. For example, de Swaan [1976] suggests that observations of the pressure drawdown in the first few hours of production can be used to estimate two important expressions, $k_{fr}w$ and k_pD. Results from well tests can be used with permeability estimates and estimates of fracture spacing based on the examination of cores and well logs, to estimate the thermal depletion due to fractures.

One additional application of our model is in the study of the hot-dry-rock concept. It has been suggested [Harlow and Pracht, 1972; Austin, 1973; Bodvarsson, 1969; Gringarten el al., 1975] that by injecting cold water into one (or more) artificially produced fractures in hot, impermeable rock,

thermal stress cracking might be produced which would provide sufficient additional surface area to prevent rapid heat depletion at production wells. Assuming that thermal stress cracking does occur, one could assign time-dependent values to the fracture permeability and the thermal mass in the rubble-filled fracture zone and do a depletion study for assumed system configurations using our model.

SUMMARY

Fractures are often an attractive drilling target in geothermal areas because they allow a high flow rate per well. However, fracture systems linking the injection and production wells may lead to a rapid temperature decline at the production well. We have presented a method for estimating the extent to which different fracture systems may shorten the useful lifetime of a geothermal well.

ACKNOWLEDGMENTS

The authors wish to acknowledge the help of many Lawrence Livermore Laboratory colleagues, especially J. H. Howard and J. F. Schatz. We also thank W. E. Brigham for encouraging comments.

This work was performed under the auspices of the U.S. Energy Research and Development Administration under contract No. W-7405-Eng-48.

REFERENCES

AUSTIN, A. L., Comments on a paper by F. H. Harlow and W. E. Pracht, Lawrence Livermore Lab. Rept. UCRL-7478, 1973.

BOVARSSON, G., Geothermal resource energetics, Geothermics, 3, 83, 1974.

BODVARSSON, G., On the temperature of water flowing through fractures, J. Geophys. Res., 74, 1987, 1969.

BROWNELL, D. H., JR., S. K. GARG, and J. W. PRITCHETT, Computer simulation of geothermal reservoirs, paper presented at the 45th Annual Calif. Regional Mtg., Soc. Petrol. Eng., Amer. Inst. Mining Eng., Ventura, Calif., April 1975.

CARSLAW, H. S. and J. C. JAEGER, Conduction of Heat in Solids, 2nd ed., Clarendon Press, Oxford, 1959.

de SWAAN, A., Analytic solutions for determining naturally fractured reservoir properties by well testing. Soc. Petrol. Eng. J., 16, 117, 1976.

DUTCHER, W. F. HARDT, and W. R. MOYLE, Preliminary appraisal of ground water in storage with reference to geothermal resources in the Imperial Valley area, California, U.S. Geol. Survey Circ. 649, 1972.

GRINGARTEN, A. C., P. A. WITHERSPOON, and Y. ONISHI, Theory of heat extraction from fractured hot dry rock, J. Geophys. Res., 80, 1120, 1975.

HARLOW, F. H. and W. E. PRACHT, A theoretical study of geothermal energy extraction, J. Geophys. Res., 77, 7038, 1972.

HELGESON, H. C., Geologic and thermodynamic characteristics of the Salton Sea geothermal system, Amer. J. Sci., 266, 129, 1968.

HILL, D. P., P. MOWINCKEL, and L. G. PEAKE, Earthquakes, active faults, and geothermal areas in the Imperial Valley, California, Science, 188, 1306, 1975.

HOMSY, G. M., Problems in modeling front propagation in in situ coal processing, Lawrence Livermore Lab. Rept. UCID-16897, 1975.

KEENAN, J. H., F. G. KEYES, P. G. HILL, and J. G. MOORE, Steam Tables — Thermodynamic Properties of Water Including Vapor, Liquid, and Solid Phases, Metric Units, John Wiley & Sons, New York, 1969.

LAMB, H., Hydrodynamics, 6th ed., Dover Press, New York (1932).

LASSETER, T. L., P. A. WITHERSPOON, and M. J. LIPPMANN, Multiphase, multidimensional simulation of geothermal reservoirs, paper presented at the 2nd UN Symposium on the Development and Use of Geothermal Resources, San Francisco, California, May 1975.

MATTHEWS, C. S., and D. G. RUSSELL, Pressure Buildup and Flow Tests in Wells, Soc. Petrol. Eng. AIME, New York, 1967.

MEIDAV, T., R. WEST, A. KATZENSTEIN, and Y. ROTSTEIN, An electrical resistivity survey of the Salton Sea geothermal area, Imperial Valley, California, Lawrence Livermore Lab. Rept. UCRL-13690, 1976.

MERCER, J. JR., Finite element approach to the modeling of hydrothermal systems, Ph.D. Thesis, University of Illinois, Urbana, 1973.

RANDALL, W., An analysis of the subsurface structure and stratigraphy of the Salton Sea geothermal anomaly, Imperial Valley, California, Ph.D. Thesis, University of California, Riverside, 1974.

SCHROEDER, R., Reservoir engineering report for the Magma-SDG&E geothermal experimental site near the Salton Sea, California, Lawrence Livermore Lab. Rept. UCRL-52094, 1976.

SOMERTON, W. H., Some thermal characteristics of porous rocks, Trans. Soc. Petrol. Eng. AIME, 213, 375, 1958.

SOMERTON, W. H. and G. D. BOOZER, Thermal characteristics of porous rocks at elevated temperatures, Trans. Soc. Petrol. Eng. AIME, 219, 418, 1960.

TOWSE, D., An estimate of the geothermal energy resource in the Salton Trough, California, Lawrence Livermore Lab. Rept. UCRL-51851, 1975.

TOWSE, D., and T. PALMER, Summary of geology at the ERDA-Magma-SDG&E geothermal test site, Lawrence Livermore Lab. Rept. UCID-17008, 1976.

WHITING, R. L., and H. J. RAMEY, JR., Application of material and energy balance to geothermal steam production, J. Petrol. Technol., 20, 893, 1969.

KSM/gw/aj/gw

APPENDIX A. SOLUTION OF COUPLED LINEAR EQUATIONS FOR THE CASE OF CONSTANT COEFFICIENTS.

Equations (27) can be expressed in the following form:

$$\frac{dx}{dt} = -a_1 x + a_2 y + a_B \tag{A1}$$

$$\frac{dy}{dt} = -b_2 y + b_2 x + b_3 \tag{A2}$$

Differentiation and rearrangement gives

$$\frac{d^2x}{dt^2} = + (a_{1+}b_1) \frac{dy}{dt} + (b_1 a_1 - a_2 b_2) = 0 \tag{A3}$$

$$\frac{d^2y}{dt^2} = + (a_1+b_1) \frac{dy}{dt} + (b_1 a_1 - a_1 - a_2 b_2) = 0 \tag{A4}$$

The solution for x is

$$x(t) = A_x e^{M_1 t} + B_x e^{M_2 t} \tag{A5}$$

where

$$M_{1,2} = -\frac{a_1+b_1}{2} \pm \frac{1}{2} \sqrt{(a_1+b_1)^2 - 4(b_1 a_1 - a_2 b_2)} \tag{A6}$$

A_x and B_x are determined from the initial conditions on x and equation (A5).

$$x(0) = A_x + B_x$$

$$\left.\frac{dx'}{dt}\right|_{t=0} = -a_1 x'(0) + a_2 y'(0) = m_1 A_x + m_2 A_y$$

The solution for y is determined in a similar fashion.

TABLE 1. The Salton Sea (SSGF) reservoir parameter values and initial conditions.

Parameter	Units	Ref.*	Parameter	Units	Ref.*
$\rho_f = 1000$	kg/m^3	H	$T_0 = 573$	K	H
$\rho_s = 2200$	kg/m^3	**	$T_{ref} = 323$	K	**
$C_f = 4.8 \times 10^3$	J/kg•K	K	$\phi = 0.16$		D, H
$C_s = 1.1 \times 10^3$	J/kg•K	S	$V_R = 8.1 \times 10^{9}$†	m^3	T
$K_f = 0.55$	W/m•K	K	$k_p = 1. \times 10^{-13}$	m^2	Sc
$K_s = 3.3$	W/m•K	S	$q = 2.22 \times 10^3$	kg/s	**

*D refers to Dutcher et al. [1972];
H refers to Helgeson [1968];
K refers to Keenan et al. [1969];
Sc refers to Schroeder [1967];
S refers to Somerton [1958] and Somerton and Bauzer [1960];
T refers to Towse [1975].

**Estimated value.

†V_R = MV, which is the total volume of the reservoir.

FIGURE CAPTIONS

Fig. 1. A qualitative view of the heat budget for geothermal reservoir depletion with rock/fluid heat flow and constant reservoir mass.

Fig. 2. A qualitative view showing the fluid flow path after separation of the reservoir into M regions. In each region, the average temperature of each of two components (saturated rock and fracture fluid) is computed. Mixing of fracture fluid and pore fluid in space between regions is optional.

Fig. 3. (a) Slab model of a region of rock with fractures indicating faces through which heat conduction and fluid flow are allowed. The wells are vertical for this example. (b) Subdivision of region into small blocks in which the temperature variables are assumed not to change in the direction of fluid flow within the block.

Fig. 4. Calculated depletion curves for reservoirs with no fractures. The step function is the analytical solution.

Fig. 5. Comparison of our calculated curves (dashed) with those of Gringarten et al. [1975] (solid). Their values have been converted to our dimensionless format.

Fig. 6. Thermal depletion curves for different fracture spacings D (in meters). Table 1 gives the reservoir parameters used in the calculations. The flow rate and fracture aperture ($w = 0.003$ m) are the same for all curves. Because a high permeability was chosen ($k_p = 10^{-13}$ m^2), unrealistically large values of D are necessary to illustrate the increased lifetime for very large fracture spacings.

Fig. 7. Contour plots of the correction factor to be used if reservoir lifetime (τ) based on flow in porous media is (a) 6.6 years, (b) 66 years, and (c) 666 years. Physical properties are given in Table 1. Use of this figure for systems with different physical properties is discussed in the text. (d) Location of lines of constant D and w (both in meters) on R_q-vs-R_μ plot, for physical parameters of Salton Sea, assuming $k_{fr} = w^2/12$. Shaded area shows range of D and w where porous flow calculations are essentially correct. ($t_L/\tau \geq 0.5$.)

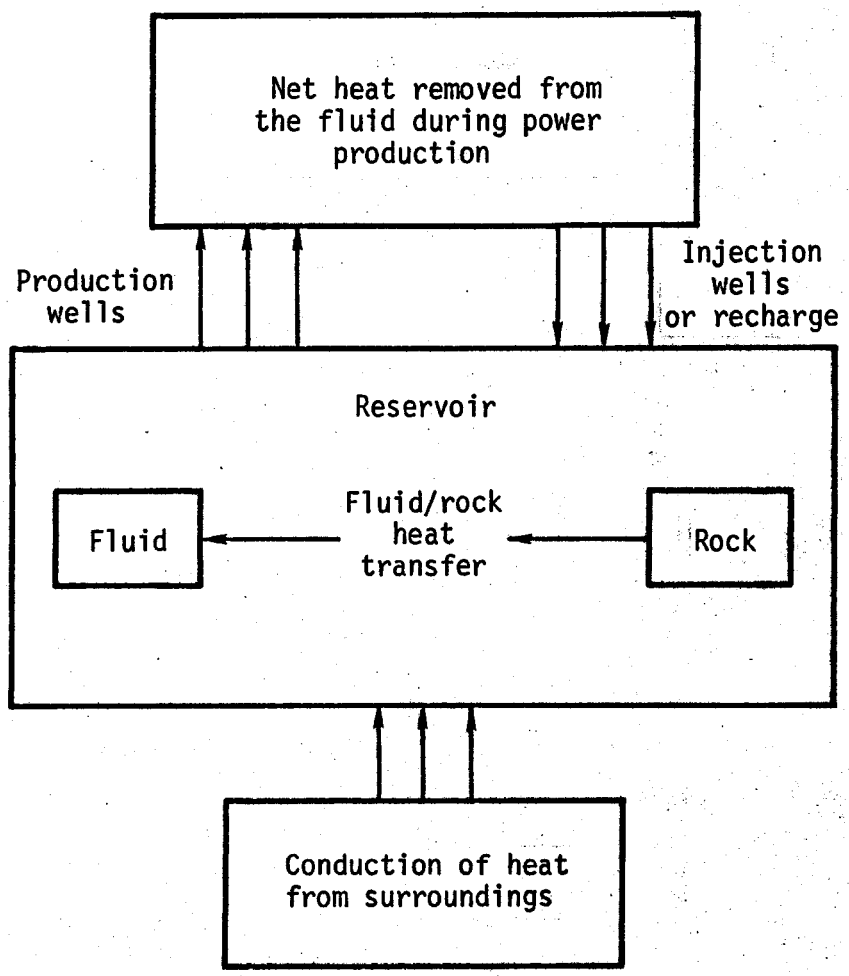

Kasameyer - Fig. 1

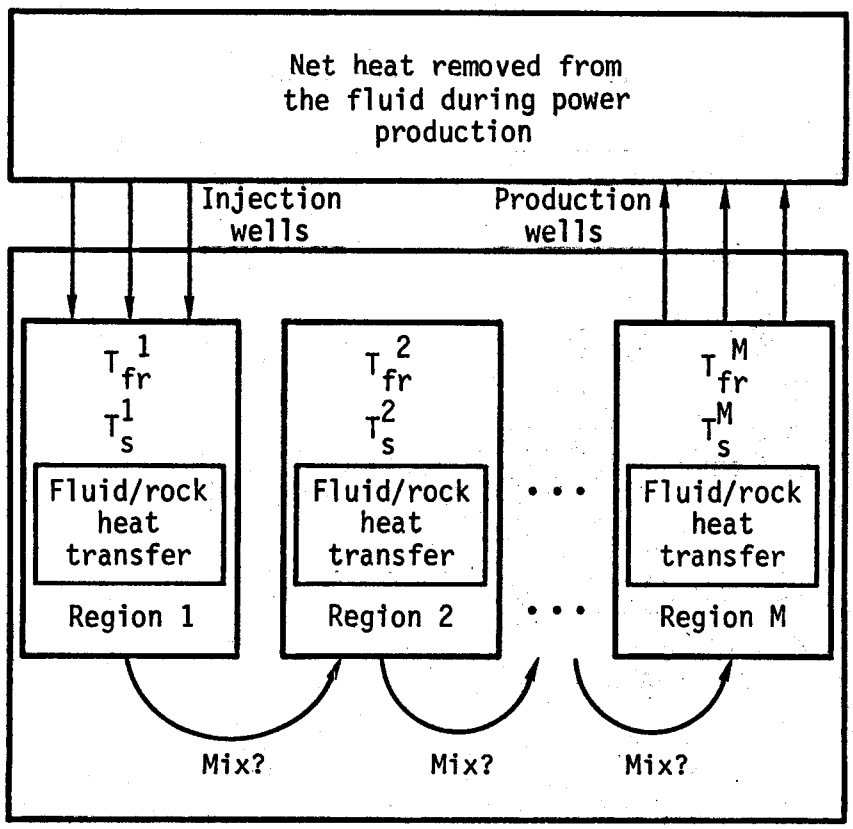

Kasameyer - Fig. 2

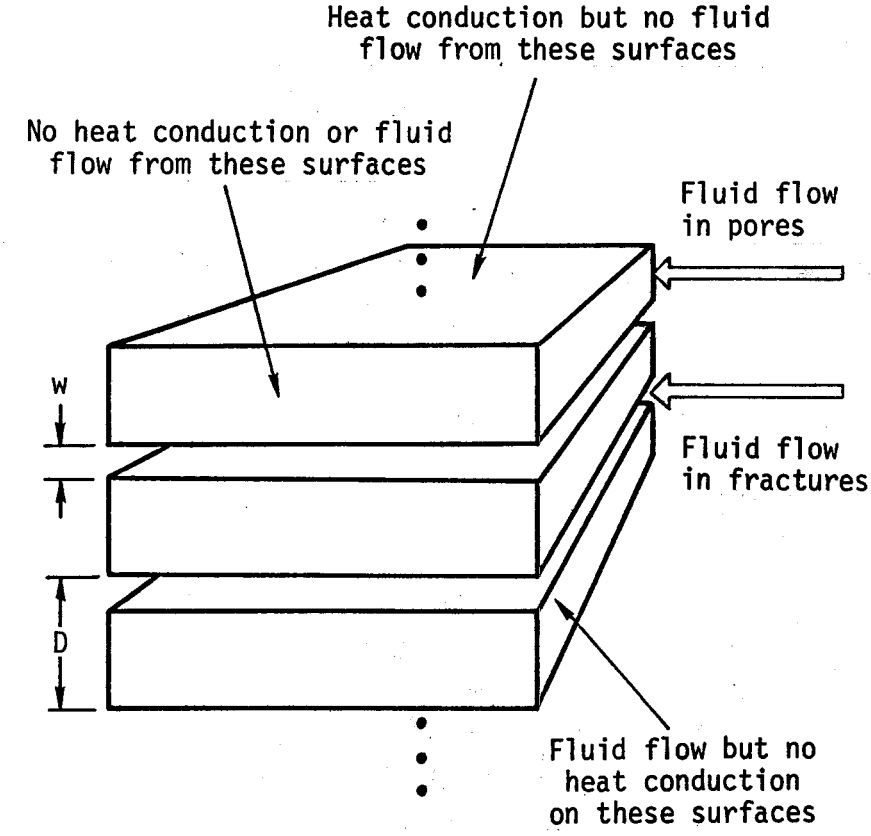

(a)

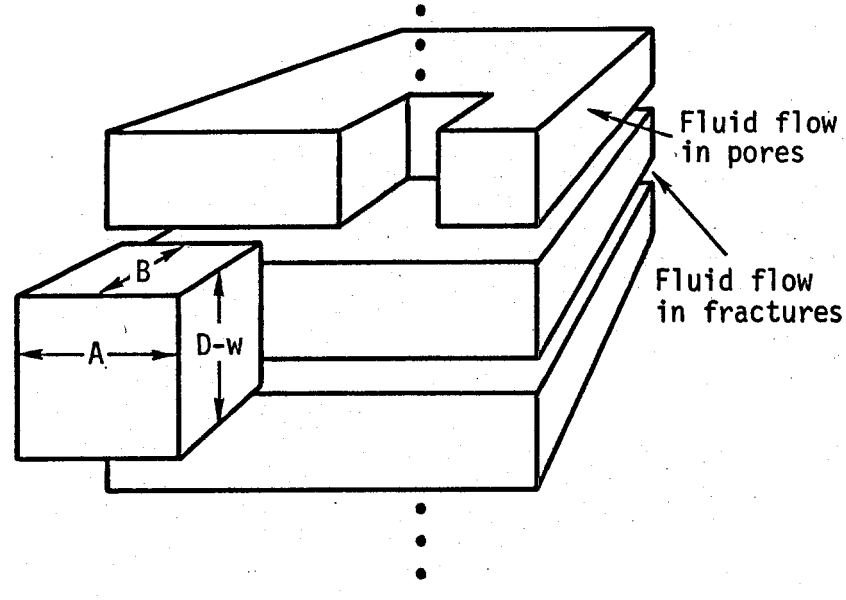

(b)

Kasameyer - Fig. 3

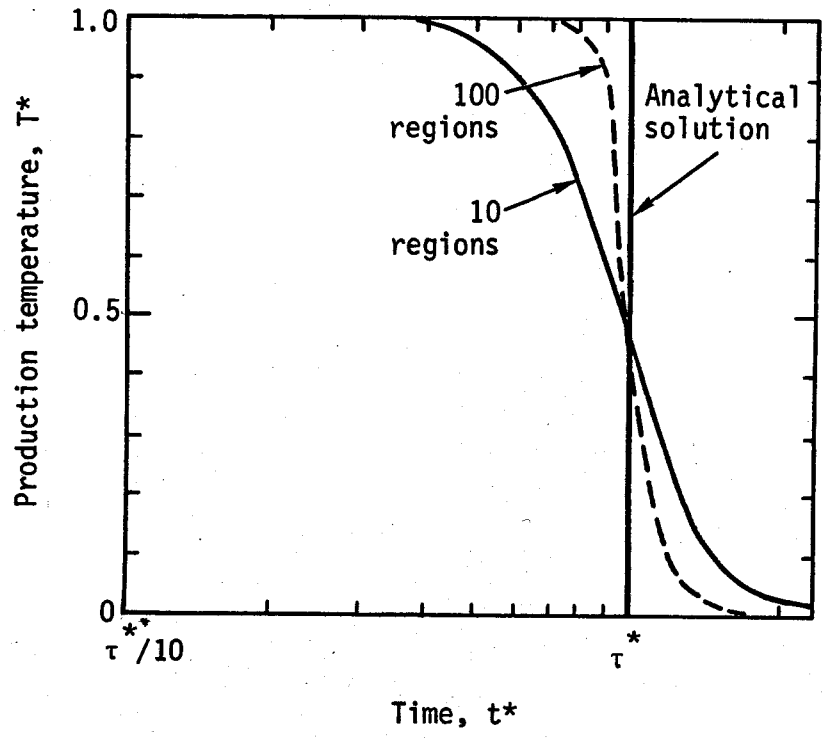

Kasameyer - Fig. 4

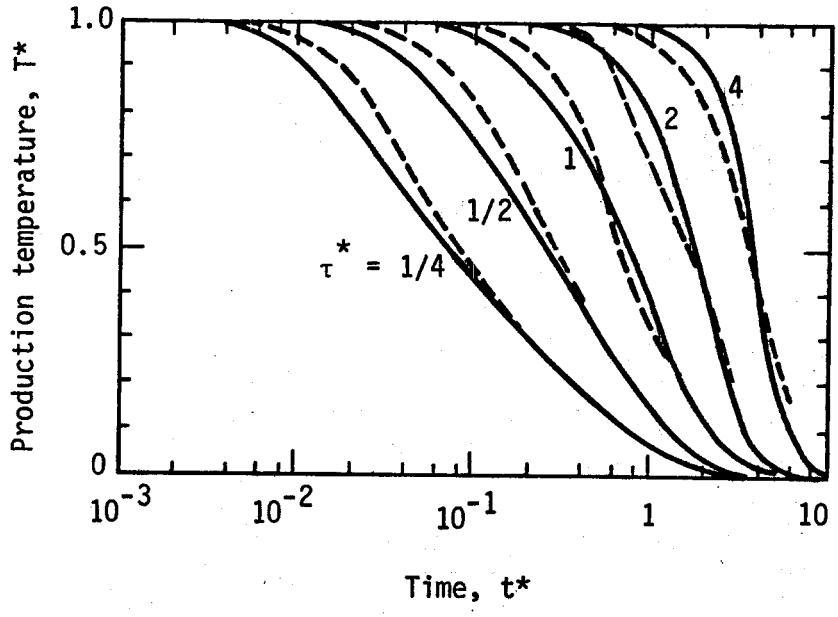

Kasameyer Fig. 5

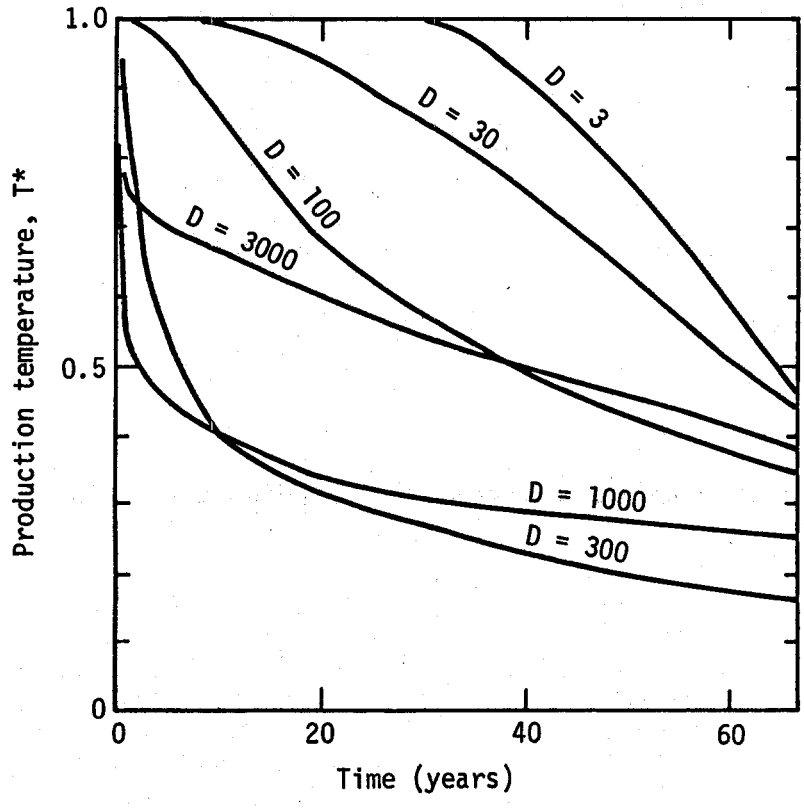

Kasameyer - Fig. 6

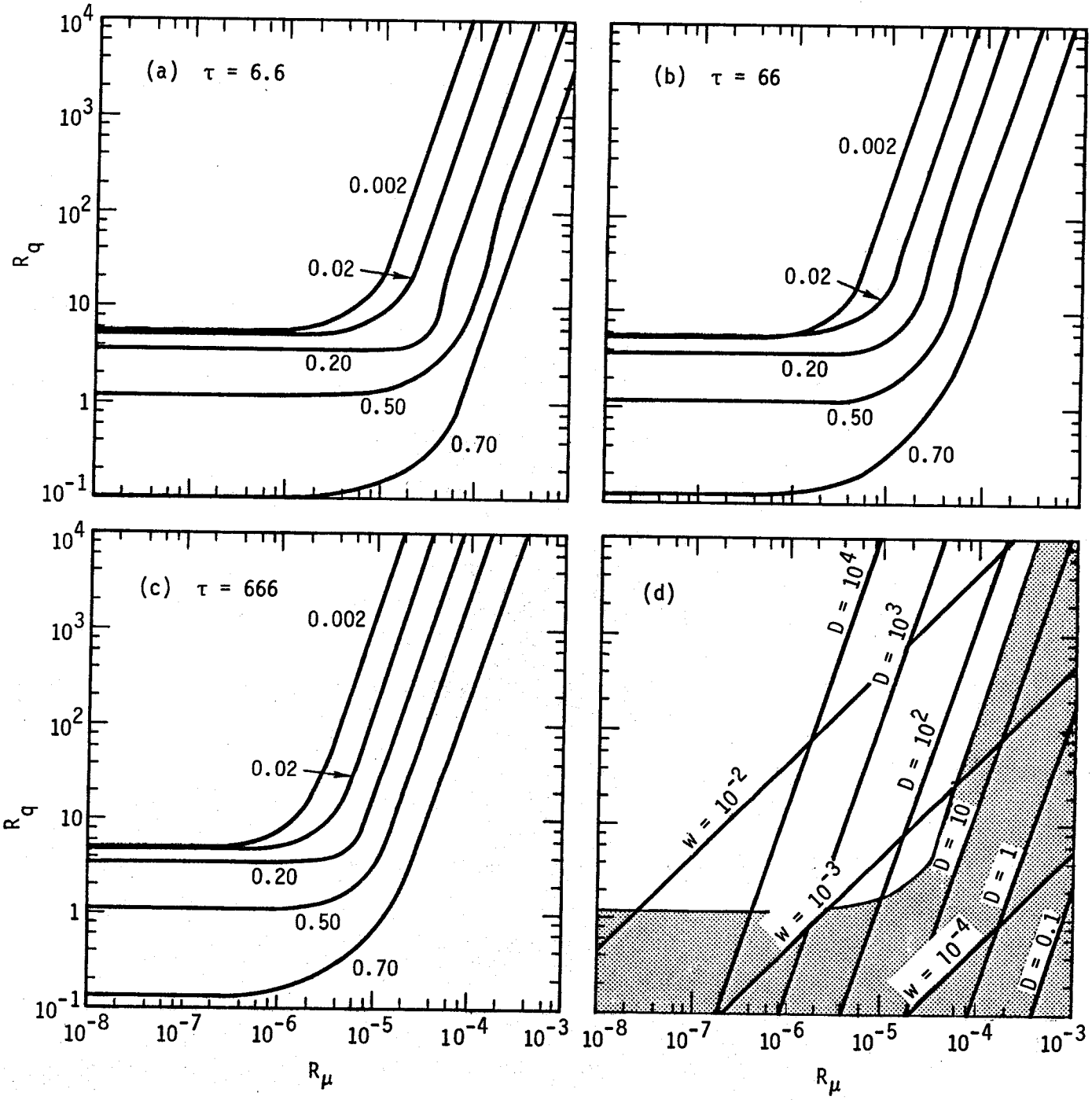

Kasameyer - Fig. 7